Dynamic Task/Posture Decoupling for Minimally Invasive Surgery Motions

Micaël Michelin, Philippe Poignet, Etienne Dombre

Dynamic Task / Posture Decoupling for Minimally Invasive Surgery Motions

Micaël Michelin, Philippe Poignet, Etienne Dombre

LIRMM – UMR 5506 CNRS / Université Montpellier II
Montpellier, France
michelin@lirmm.fr, poignet@lirmm.fr, dombre@lirmm.fr

Abstract. This paper deals with the use of an original dynamic task / posture decoupling control algorithm that allows a robot to achieve motions under the constraint of moving through a fixed point. This work takes place in the context of minimally invasive surgery where the tool is telemanipulated by the surgeon through a penetration point: the trocar fixed on the patient. The algorithm is based on the dynamic control in the operational space of a redundant robot: the total control torque is decoupled into a task behavior torque and a posture behavior torque. By minimizing the contact force applied to the trocar (or equivalently, by forcing to zero the distance between the instrument passing through the trocar and the current location of the trocar), we compute the posture behavior torque guaranteeing that the trocar constraint is satisfied. Implementation on a real robot has been done. Experimental results highlight the performance of this algorithm when the instrument tip follows various paths such as straight lines, circles and helices.

1 Introduction

In the ten past years, minimally invasive surgery (MIS) has become widespread in surgical operations. MIS consists in achieving operation through small penetration points in the body equipped with trocars. The surgeon uses dedicated instruments consisting in a long tube (30 – 40 cm) with a tool fixed at one end and a handle fixed at the other. MIS adds several difficulties in the surgical procedure. An important one is that the penetration point reduces the tool orientation capabilities and the amplitude of motion.

After training, the surgeon can overcome these difficulties in most abdominal operations. However, for microsurgery or cardiac surgery, it is necessary to make use of a robot working in a teleoperated mode. The surgeon can then focus on the tool motion rather than on the complex motion of the arm due to the constraint.

A few robotic systems have been designed to assist surgeons, such as Zeus from Computer Motion or Da Vinci from Intuitive Surgical. The main feature of these systems is to mechanically create a fixed point that coincides with the penetration point. Zeus makes use of a passive universal joint [1]. Da Vinci and other prototypes such as FZK Artemis and UCB/UCSF RTW systems are designed as remote center devices [2][3][4][5]. Another way to create a fixed point is to implement an appropriate force-position control. The tool is position-controlled within the patient while respecting a force constraint on the trocar [6]. Finally, let

us mention a hybrid system consisting of a parallel structure outside the patient holding a serial structure located inside [7].

In this paper, we propose a novel approach based on the dynamic decoupling of the control torque into a task behavior control and a posture behavior control. In fact, by minimizing the contact force or, equivalently, by forcing to zero the distance between the instrument passing through the trocar and the current location of the trocar (or the desired location, if the goal is to control it), we compute the posture behavior torque as the gradient of a cost function representing the distance. This approach allows us to control the penetration point required during MIS. It has been on a real five degree-of-freedom (dof) robot, which achieves motion under the constraint of passing the instrument through a fixed penetration point.

The paper is organized as follows: section 2 recalls the dynamics formulation, the principle of task / posture decoupling, and the proposed algorithm. In section 3, we present the robot D2M2 dedicated to beating heart surgery, as well as the first experimental results obtained when the tip of the surgical instrument is programmed to follow paths such as straight lines, circles and helices.

2 Task / posture dynamic decoupling

2.1 Joint space and operationnal space dynamics

The joint space dynamic model for a N-dof open-chain manipulator is given by

$$\Gamma = \mathbf{A}(\mathbf{q})\ddot{\mathbf{q}} + \mathbf{b}(\mathbf{q},\dot{\mathbf{q}}) + \mathbf{g}(\mathbf{q}) \tag{1}$$

where $\mathbf{A}(\mathbf{q})$ is the NxN joint space inertia matrix, $\mathbf{b}(\mathbf{q},\dot{\mathbf{q}})$ is a Nx1 vector combining joint space Coriolis forces and centrifugal forces, and $\mathbf{g}(\mathbf{q})$ is the Nx1 joint space gravitational force vector.

The operational space behavior is given by

$$\mathbf{F} = \Lambda(\mathbf{q})\ddot{\mathbf{X}} + \mu(\mathbf{q},\dot{\mathbf{q}}) + \rho(\mathbf{q}) \tag{2}$$

where $\Lambda(\mathbf{q})$, $\mu(\mathbf{q},\dot{\mathbf{q}})$ and $\rho(\mathbf{q})$ represent respectively the inertia matrix, the Coriolis / centrifugal force vector and the gravity force vector in the operational space [9].

2.2 Joint space and operationnal space correspondance

Joint space and operational space are related by the following expressions [10]

$$\Lambda(\mathbf{q}) = (\mathbf{J}(\mathbf{q})\mathbf{A}^{-1}(\mathbf{q})\mathbf{J}^{T}(\mathbf{q}))^{-1} \tag{3}$$

$$\mu(\mathbf{q},\dot{\mathbf{q}}) = \bar{\mathbf{J}}^{T}(\mathbf{q})\mathbf{b}(\mathbf{q}) - \Lambda(\mathbf{q})\dot{\mathbf{J}}(\mathbf{q})\dot{\mathbf{q}} \tag{4}$$

$$\rho(\mathbf{q}) = \bar{\mathbf{J}}^{T}(\mathbf{q})\mathbf{g}(\mathbf{q}) \tag{5}$$

where $\bar{\mathbf{J}}(\mathbf{q})$ is the dynamically consistent generalized inverse of the Jacobian matrix $\mathbf{J}(\mathbf{q})$ that links joint velocities and operational velocities such that

$$\dot{\mathbf{X}} = \mathbf{J}(\mathbf{q})\dot{\mathbf{q}} \tag{6}$$

2.3 Task and posture control torque decoupling

The control torque vector Γ applied on the joints of a redundant system can be decomposed in two contributions [10][11][12]: the first one affects the end effector position (the task control torque Γ_{task}), the other one allows to change the joint configuration without any end effector motion (the posture control torque $\Gamma_{posture}$)

$$\Gamma = \Gamma_{task} + \Gamma_{posture} \tag{7}$$

The task control torque Γ_{task} that acts in the operational space is given by

$$\Gamma_{task} = J^T F \tag{8}$$

where F is the force vector acting on the robot in the operational space.

The posture control torque $\Gamma_{posture}$ generating joint motion without any operational motion is expressed as

$$\Gamma_{posture} = (I_N - J^T \bar{J}^T)\Gamma_{null} \tag{9}$$

where Γ_{null} is an arbitrary null space control torque vector that is chosen by the user, and $I_N - J^T \bar{J}^T$ is an appropriate projection matrix that maps Γ_{null} to the control torque. Γ_{null} can be written as

$$\Gamma_{null} = A\ddot{q}_{null} + b + g \tag{10}$$

where $\ddot{q}_{null}$ is the null space posture behavior.

By developing (7) and combining it with (1), (2), (3), (4) and (5), it follows that (see appendix for computation details)

$$\Gamma = J^T \Lambda(\ddot{X} - \dot{J}\dot{q} - J\ddot{q}_{null}) + \Gamma_{null} \tag{11}$$

2.4 Minimally invasive surgery context

MIS operations constrain the instrument manipulated by the surgeon to pass through a fixed penetration point. As explained in section I, existing medical devices such as Da Vinci or Zeus satisfy this constraint thanks to a dedicated kinematic design. We propose to use the decoupling control presented above to meet this goal with a redundant kinematic architecture.

2.5 Optimization

The task / posture dynamic decoupling algorithm detailed above offers the possibility of utilizing the null space to optimize an objective function associated to the computation of the arbitrary control torque Γ_{null}. In the context of minimally invasive surgery, Γ_{null} will be computed in order to force to zero the distance between the instrument and a given location of the trocar. It will result in internal joint motions guaranteeing that the instrument will respect the penetration point constraint.

In [8], the use of the optimization term of the inverse kinematic general solution allows to optimizing internal motions to achieve secondary tasks such as

staying away from the joint limits. In our case, we choose the control torque Γ_{null} as the gradient $\nabla_{\mathbf{q}}\phi(\mathbf{q})$ of a scalar positive definite function $\phi(\mathbf{q})$ of the joint position balanced by a negative term α that ensures the decreasing of $\phi(\mathbf{q})$. If this function is expressed as the projection of the penetration point on the instrument held by the robot, then the global control torque forces the robot to decrease this distance, and thus to respect the constraint. Given

$$\Gamma_{null} = \alpha\nabla\phi \tag{12}$$

the expression of the global torque is

$$\Gamma = \mathbf{J}^T\mathbf{F} + (\mathbf{I}_N - \mathbf{J}^T\bar{\mathbf{J}}^T)\alpha\nabla\phi \tag{13}$$

where

$$\nabla\phi(\mathbf{q}) = [\frac{\partial\phi(\mathbf{q})}{\partial\mathbf{q}_1} \cdots \frac{\partial\phi(\mathbf{q})}{\partial\mathbf{q}_N}]^T \tag{14}$$

The expression (11) can be written as

$$\Gamma = \mathbf{J}^T\Lambda(\ddot{\mathbf{X}} - \dot{\mathbf{J}}\dot{\mathbf{q}} - \mathbf{J}\mathbf{A}^{-1}(\alpha\nabla\phi - \mathbf{b} - \mathbf{g})) + \alpha\nabla\phi \tag{15}$$

Fig. 1 illustrates the control scheme: the input $\mathbf{X}^d$ is the desired tool position and the input $\mathbf{X}_{Tr}$ corresponds to the penetration point position, assumed to be fixed in the base frame. A proportional-derivative control is used for controlling the instrument.

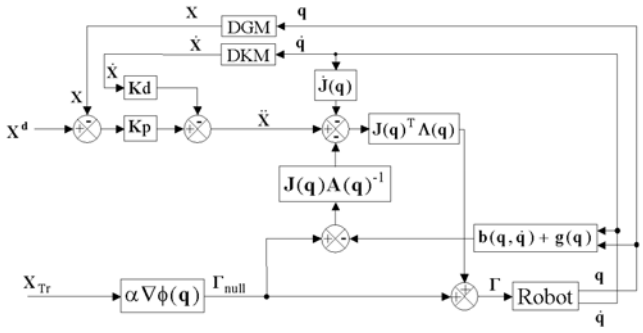

Fig. 1. Dynamic decoupling scheme. DGM and DKM stand respectively for direct geometric and kinematic models.

3 Experimental results

3.1 Experimental platform

We have implemented the algorithm on the D2M2 (Direct Drive Medical Manipulator) robot. This robot has been designed for beating heart MIS (**Fig. 2**). It is equipped with direct drive actuators to provide high dynamics. The controller is a Pentium III 500 MHz with 256 Mo RAM PC running under RTX/Windows 2000. The sample rate is 1 KHz. D2M2 may be teleoperated via UDP communication from a PHANTOM 1.5 arm working as a master device under Windows XP.

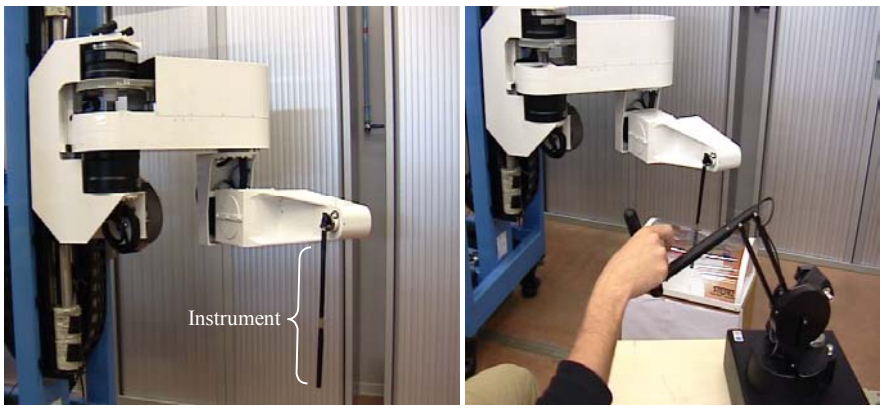

Fig. 2. The 5-dof robot D2M2 and the PHANTOM master device

The kinematic structure of D2M2 is given in **Fig. 3**. The first joint is a translation, the two following ones are rotations with scara disposition, both last are rotation laid out with 90° between them.

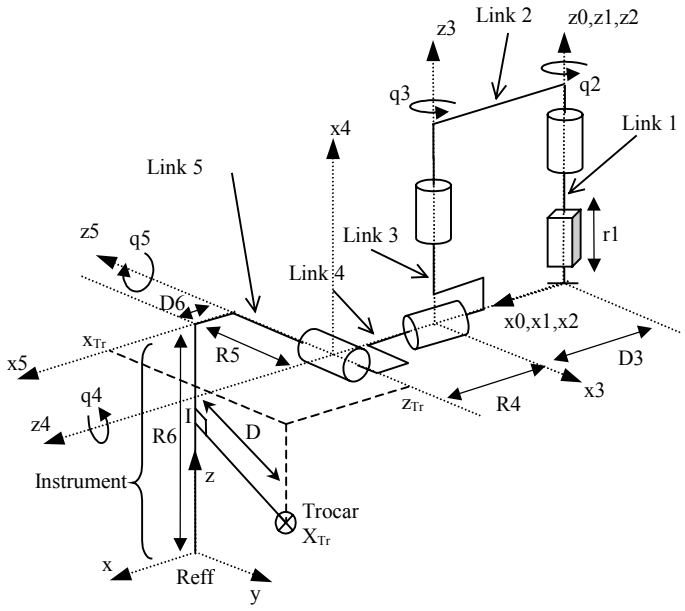

Fig. 3. Kinematic structure of D2M2.

The modeling is computed with the SYMORO (SYmbolic MOdeling of RObots) software[1] from the geometrical Denavit-Hartenberg parameters given in

[1] Developed by IRCyN (Institut de Recherche en Cybernetique de Nantes).

Fig. 4 and dynamic parameters given in **Fig. 5** obtained from CAD software. The units used are the SI units: distance in m (Dj, Rj), mass (Mj) in Kg, moment of inertia (XXj, YYj, ZZj) in Kg.m^2, first moment of inertia (MXj, MYj, MZj, IAj) in Kg.m, forces (FSj) in N, viscous forces (FVj).

Joint j	Type	σj	αj	dj	θj	rj
1	P	1	0	0	0	r1
2	R	0	0	0	q2	0
3	R	0	0	D3 = 0.4	q3 + π/2	0
4	R	0	π/2	0	q4 + π/2	R4 =0.451
5	R	0	-π/2	0	q5 - π//2	R5 = 0
Reff			-π//2	D6	0	-R6 = -0.405

Fig. 4. D2M2 geometrical Denavit-Hartenberg parameters

M1 = 17.122	M3 = 1.654	XX4 = 0.726	ZZ5 = 0.0187
IA1 = 4	ZZ3 = 0.0232	YY4 = 0.726	MX5 = 0
FV1 = 1	MY3 = 0.109	ZZ4 = 0.0117	MY5 =-0.075
FS1 = 0	IA3 = 0.012	ZZ4 = 0.0009	MZ5 = 0
M2 = 7.726	FV3 = 0.5	IA4 = 0.0025	IA5 = 0.0025
ZZ2 = 0.359	FS3 = 0	FV4 = 0.05	FV5 = 0.0500
MX2 = 1.684	M4 = 6.123	FS4 = 0	FS5 = 0
IA2 = 0.015	MX4 = 0	M5 = 0.3	
FV2 = 0.9	MZ4 = -2.109	XX5 = 0.018	
FS2 = 0	MY4 =-0.075	YY5 = 0	

Fig. 5. D2M2 dynamic parameters

3.2 Cost function

The function ϕ is chosen as the square of the distance D between the fixed penetration point (trocar position $\mathbf{X}_{Tr}$) and the instrument held by the robot (**Fig. 3**). This function, depending on $\mathbf{q}$ and $\mathbf{X}_{Tr}$, is expressed in the frame 5 by:

$$\begin{aligned} &\phi(\mathbf{q},\mathbf{X}_{Tr}) = \mathbf{D}(\mathbf{q},\mathbf{X}_{Tr})^2 \\ &\phi(\mathbf{q},\mathbf{X}_{Tr}) = ({}^5x_I(\mathbf{q},\mathbf{X}_{Tr}) - {}^5x_{Tr})^2 + ({}^5y_I(\mathbf{q},\mathbf{X}_{Tr}) - {}^5y_{Tr})^2 + ({}^5z_I(\mathbf{q},\mathbf{X}_{Tr}) - {}^5z_{Tr})^2 \end{aligned} \quad (16)$$

where subscript I denotes the projection of the trocar position on the instrument.

3.3 Real implementation

Classical trajectories for MIS such as straight line, circle and helix paths have been performed (**Fig. 6**).

Fig. 6. Straight line motion of D2M2 under constraint of trocar

The gains of the control algorithm have been tuned from simulation results to:

- **Kp** = 3000
- **Kd** = 25
- $\alpha = -4600$

A 20 cm straight line is experimented first; the **Fig. 7**.left shows a tracking error less than 2.10^{-2} m and the distance between the trocar and the instrument stay less than 2.10^{-2} m (**Fig. 7**.right). The maximum speed and the acceleration reached by the tool are respectively 0.16 $m.s^{-1}$ and 0.25 $m.s^{-2}$. The generated torques (**Fig. 8**) remain within the range of capabilities of motors but they are very unstable in certain positions of the robot.

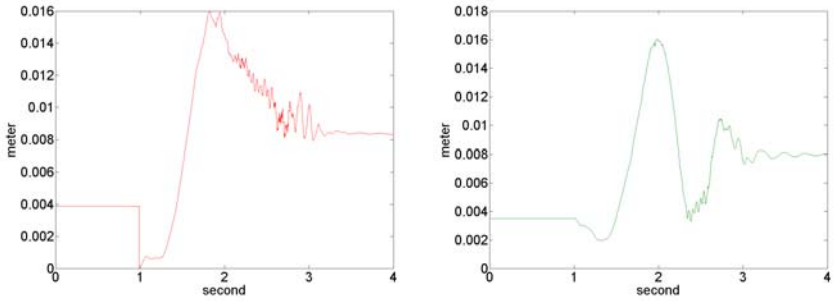

Fig. 7. Tracking error (left) and distance trocar–instrument (right) during straight line motion.

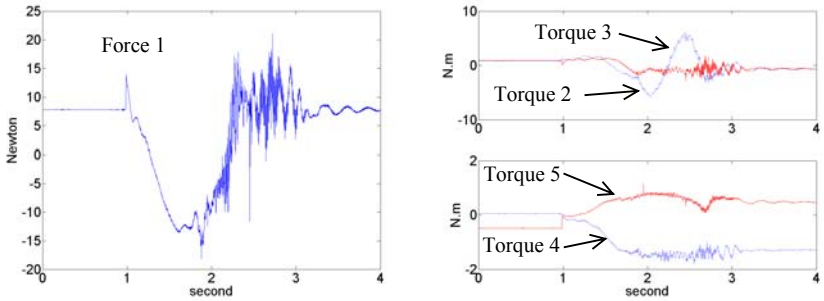

Fig. 8. Force and torques during straight line motion.

Circular paths of 10 cm diameter (**Fig. 9** and **Fig. 10**) and helicoid path with 2 cm pitch (**Fig. 11** and **Fig. 12**) have been achieved. The results are similar to those obtained with straight line.

The instabilities appearing in the results are due to the noise on the measures of the joints position.

3.4 Discussion

Simulation results shows that D decreases significantly when the absolute value of α increases. The tracking error is not influenced by the term α, it is only tuned by the gains K_p and K_d. In simulation it can decrease less than 1 mm. However, we notice that torque oscillations increases with the absolute value of α. On the real robot, the control torques stay in reasonable physical limits. In certain joint position of robot, the control torques are very unstable. This fact is due to noise on measures and reveals a noise sensitivity of the algorithm. Data filtering have been implemented to overcome this problem. The computing time is less than 0.35 ms.

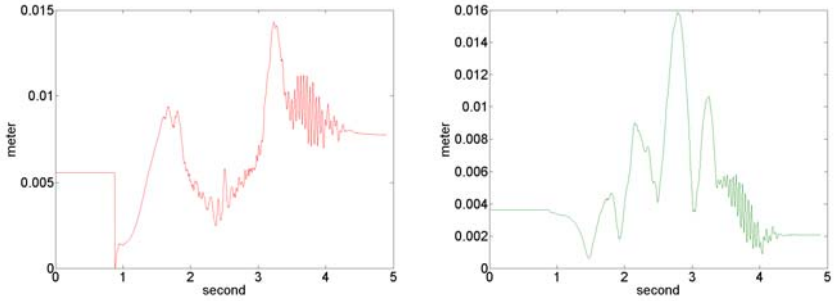

Fig. 9. Tracking error (left) and distance trocar–instrument (right) during circular motion.

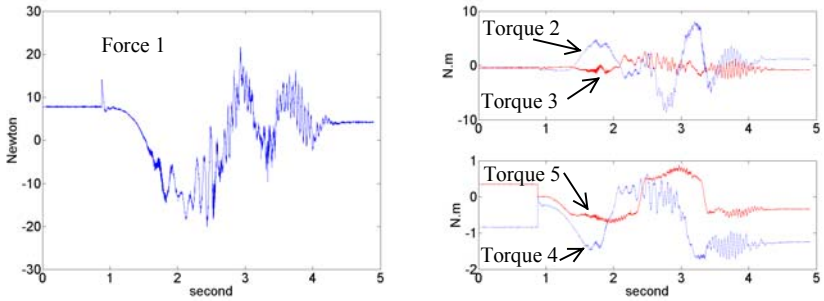

Fig. 10. Force and torques during circular motion.

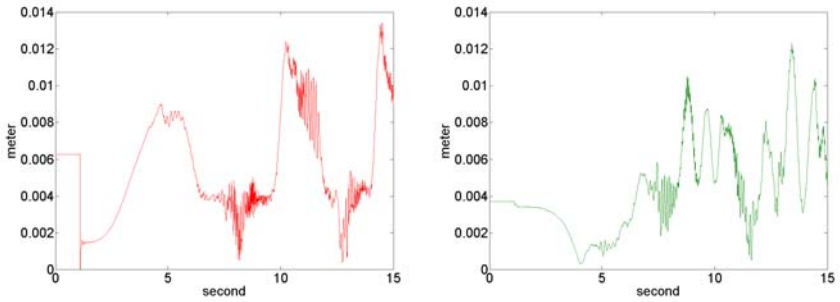

Fig. 11. Tracking error (left) and distance trocar–instrument (right) during helix motion.

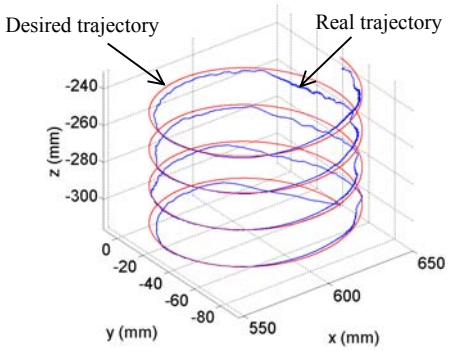

Fig. 12. Desired and real cartesian trajectories during helix motion.

4 Conclusion

We have presented an efficient dynamic decoupling control scheme based on the optimized choice of the arbitrary control torque expressed in the null space. In the context of MIS, this control allows a redundant serial robot to achieve motions guaranteeing that the instrument passes through a penetration point materializing the trocar position. The optimization term of the global solution of the static model generates internal motions that tend to reduce the distance between the trocar and the instrument. The inputs of the control structure being the end effector position and the trocar position, we have developed an efficient dynamic decoupling between the task behavior (tool motion) and the posture behavior (satisfaction of the constraint. We have validated the principle of this algorithm on the real robot D2M2.

References

[1] http://www.computermotion.com.

[2] G. Guthart, and J.K. Salisbury, "The Intuitive Telesurgery System: Overview and Applications," Proc. IEEE Int. Conf. on Robotics and Automation, San Fransisco, 2000, pp. 618-621.

[3] A.J. Madhani, G. Niemeyer, and J.K. Salisbury, "The Black Falcon: A Teleoperated Surgical Instrument for Minimally Invasive Surgery," Proc. IEEE/RSJ Int. Conf. on Intelligent Robots and Systems (IROS), Victoria B.C., Canada, October, 1998, pp. 936-944.

[4] A.J. Madhani, "Design of Teleoperated Surgical Instruments for Minimally Invasive Surgery," PhD Thesis, Massachusetts Institute of Technology, 1998.

[5] H. Rininsland, "ARTEMIS. A telemanipulator for cardiac surgery," EUROPEAN JOURNAL OF CARDIO-THORACIC SURGERY, 16: S106-S111 Suppl. 2, 1999.

[6] A. Krupa, C. Doignon, J. Gangloff, M. de Mathelin, L. Soler, and G. Morel, "Towards Semi-autonomy in Laparoscopic Surgery Through Vision and Force Feedback Control," Proc. Int. Symp. on Experimental Robotics, ISER'00, Waikiki, December 2000, pp 189-198.

[7] M.C. Cavusoglu, and F.T. Tendick, "A Laparoscopic Telesurgical Workstation," IEEE Trans. on Robotics and Automation, vol 15, no 4, 1999, pp. 728-739.

[8] W. Khalil, and E. Dombre, "Modeling, Identification and Control of Robots," Hermes Penton, London, 2002.

[9] O.Khatib, "Comande Dynamique dans l'Espace Operationnel des Robots Manipulateurs en Présence d'Obstacles," PhD Thesis, Ecole Nationale Supérieure de l'Aéronautique et de l'Espace, December 1980.

[10] O.Khatib, "A Unified Approach for Motion and Force Control of Robot Manipulators: The Operational Space Fromulation," IEEE Journal of Robotics and Automation, February 1987, RA –3(1): pp 43-53.

[11] J. Russakow, O. Khatib, and S. M. Rock, "Extended Operational Space Formulation for Serial-to-Parallel Chain (Branching) Manipulators," Proceedings of IEEE International Conference on Robotics & Automation. Nagoya, Japan, May 1995, pp. 1056-1061.

[12] K-S Chang, O Khatib, "Operational Space Dynamics: Efficient Algorithms for modeling and Control of Branching Mechanisms," Proceedings of IEEE International Conference on Robotics & Automation. San Francisco, April 2000, pp. 850-856.

Appendix

$$\Gamma = \mathbf{J}^T(\Lambda\ddot{\mathbf{X}} + \mu + \rho) + (\mathbf{I}_N - \mathbf{J}^T\bar{\mathbf{J}}^T)\Gamma_{null}$$

$$\Gamma = \mathbf{J}^T(\Lambda\ddot{\mathbf{X}} + \bar{\mathbf{J}}^T\mathbf{b} - \Lambda\dot{\mathbf{J}}\dot{\mathbf{q}} + \rho) + (\mathbf{I}_N - \mathbf{J}^T\bar{\mathbf{J}}^T)\Gamma_{null}$$

$$\Gamma = \mathbf{J}^T\Lambda\ddot{\mathbf{X}} + \mathbf{J}^T\bar{\mathbf{J}}^T\mathbf{b} - \mathbf{J}^T\Lambda\dot{\mathbf{J}}\dot{\mathbf{q}} + \mathbf{J}^T\rho + \Gamma_{null} - \mathbf{J}^T\bar{\mathbf{J}}^T\Gamma_{null}$$

$$\Gamma = \mathbf{J}^T\Lambda\ddot{\mathbf{X}} + \mathbf{J}^T\bar{\mathbf{J}}^T\mathbf{b} - \mathbf{J}^T\Lambda\dot{\mathbf{J}}\dot{\mathbf{q}} + \mathbf{J}^T\bar{\mathbf{J}}^T\mathbf{g} + \Gamma_{null} - \mathbf{J}^T\bar{\mathbf{J}}^T\Gamma_{null}$$

$$\Gamma = \mathbf{J}^T\Lambda(\ddot{\mathbf{X}} - \dot{\mathbf{J}}\dot{\mathbf{q}}) + \mathbf{J}^T\bar{\mathbf{J}}^T(\mathbf{b} + \mathbf{g}) + \Gamma_{null} - \mathbf{J}^T\bar{\mathbf{J}}^T(\mathbf{A}\ddot{\mathbf{q}}_{null} + \mathbf{b} + \mathbf{g})$$

$$\Gamma = \mathbf{J}^T\Lambda(\ddot{\mathbf{X}} - \dot{\mathbf{J}}\dot{\mathbf{q}}) + \Gamma_{null} - \mathbf{J}^T\bar{\mathbf{J}}^T\mathbf{A}\ddot{\mathbf{q}}_{null}$$

$$\Gamma = \mathbf{J}^T\Lambda(\ddot{\mathbf{X}} - \dot{\mathbf{J}}\dot{\mathbf{q}}) + \Gamma_{null} - \mathbf{J}^T\bar{\mathbf{J}}^T\mathbf{J}^T\Lambda\mathbf{J}\ddot{\mathbf{q}}_{null}$$

$$\Gamma = \mathbf{J}^T\Lambda(\ddot{\mathbf{X}} - \dot{\mathbf{J}}\dot{\mathbf{q}}) + \Gamma_{null} - \mathbf{J}^T\Lambda\mathbf{J}\ddot{\mathbf{q}}_{null}$$

$$\Gamma = \mathbf{J}^T\Lambda(\ddot{\mathbf{X}} - \dot{\mathbf{J}}\dot{\mathbf{q}} - \mathbf{J}\ddot{\mathbf{q}}_{null}) + \Gamma_{null}$$